Supporting information

Reduced Graphene Oxide Nanosheet modified NiMn-LDH nanoflake arrays for High-Performance Supercapacitors

Li Sun, Yuanxing Zhang, Yu Zhang, Haochen Si, Wenpeng Qin and Yihe Zhang**

Beijing Key Laboratory of Materials Utilization of Nonmetallic Minerals and Solid Wastes, National Laboratory of Mineral Materials, School of Materials Science and Technology, China University of Geosciences, Beijing, 100083, PR China

**E-mail: sunli@cugb.edu.cn, zyh@cugb.edu.cn*

Experimental Section

Synthesize of the NiMn-LDH@NF electrode. A homogeneous solution consisting of 4 mmol $Ni(NO_3)_2 \cdot 6H_2O$, 4 mmol $Mn(NO_3)_2 \cdot 4H_2O$, 4 mmol urea and 25 mL DI water was transferred into a 40 mL Teflon-lined stainless-steel autoclave containing one pieces of cleaned Ni foam (1×4 cm^2). The autoclave was first sealed for 1 h to ensure sufficient wetting of Ni foam by the reactant solution, and then gradually heated to 140°C and maintained for 14 h. After the autoclave cooled down, the Ni foams were washed under ultrasonication with deionized water and ethanol each for 3 times and dried at 80°C. The loading mass of active material was about 2.5 mg cm^2.

Reduced graphene oxide (rGO) modification. Graphene oxide (GO) was deposited via a simple "dip-coating" process for 3 times. The NiMn-LDH@NF electrode was immersed into a GO suspension (2 mg mL^{-1}) for 5 minutes, and then dried at 50 °C. The resultant electrode was washed with DI water and dried in air at room temperature. The as-synthesized

GO@NiMn-LDH@NF hybrid is then immersed in a hydrazine hydrate aqueous solution to obtain the rGO@NiMn-LDH@NF electrode. The mass loading of rGO was about 0.2 mg cm^{-2}. As a control sample, rGO@NF was also prepared by conducting the same procedure on Ni foam.

Material Characterizations and Electrochemical measurements. The structures of the electrodes were characterized by X-ray powder diffraction (XRD, Rigaku-D/max 2500 V), scanning electron microscopy (SEM, Sirion 200) and transmission electron microscopy (TEM, JEM 2100 F). The electrochemical performance of the electrodes was evaluated using a conventional three-electrode with Pt as the counter electrode, Ag/AgCl as the reference electrode, and 3 M KOH solution as the electrolyte. The asymmetric supercapacitor was constructed with rGO@NiMn-LDH@NF as the positive electrode and commercially obtained active carbon as the negative electrode. The asymmetric supercapacitor was assembled in a CR2016-type coin cell using 3 M KOH solution as the electrolyte, and one piece of cellulose paper as the separator. All the electrochemical tests were carried out on a CHI760E electrochemical workstation.

Supplementary Figures

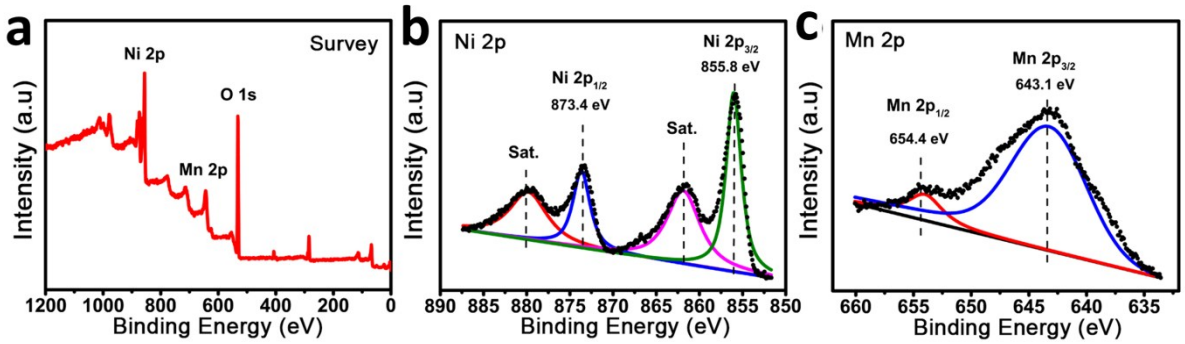

Figure S1. XPS (a) survey spectrum, and high resolution (b) Ni, (c) Mn spectra of NiMn-LDH.

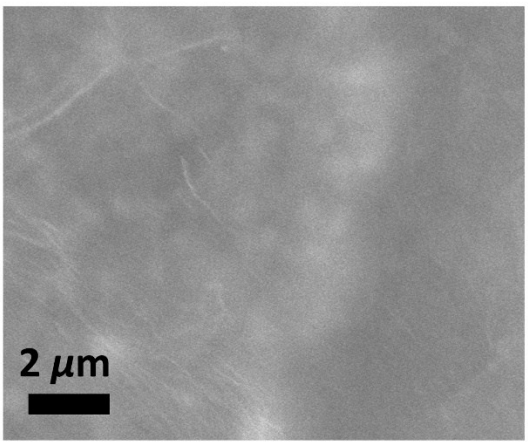

Figure S2. SEM image of rGO@NiMn-LDH@NF at high magnification.

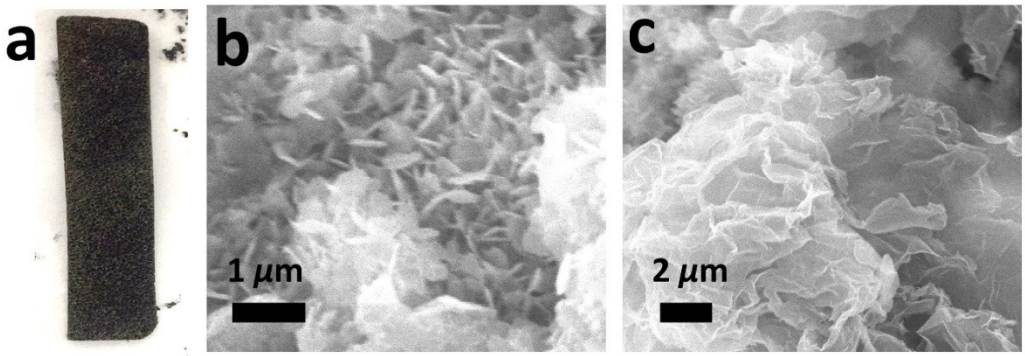

Figure S3. (a) Photo and (b, c) SEM images of the electrode surface directly modified with rGO by dip-coating method.

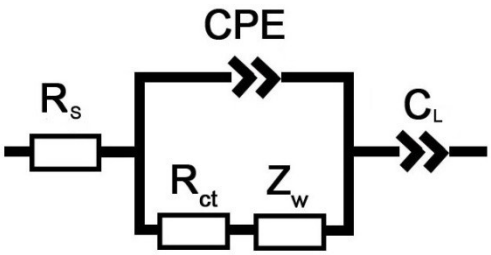

Figure S4. Equivalent circuit model of the electrodes.

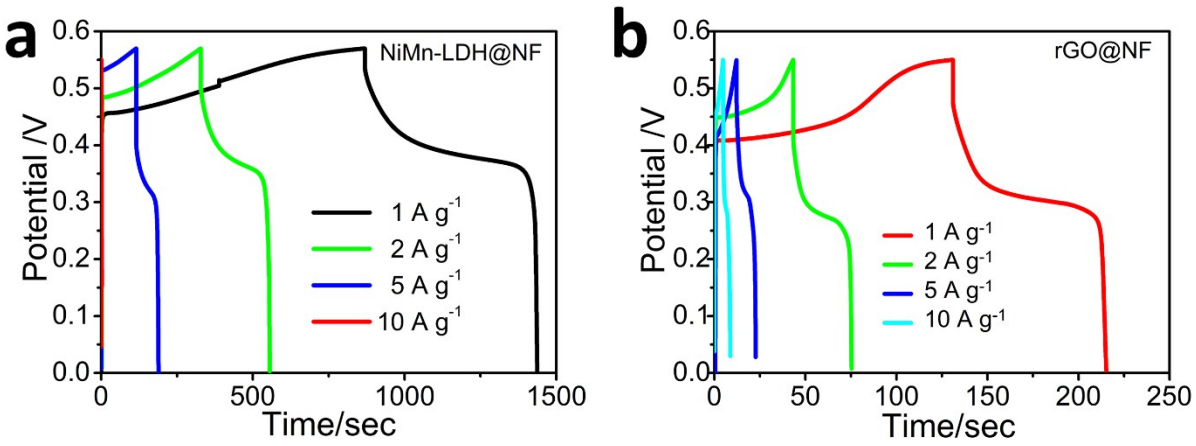

Figure S5. The galvanostatic charge-discharge curves of (a) NiMn-LDH@NF and (b) rGO@NF.

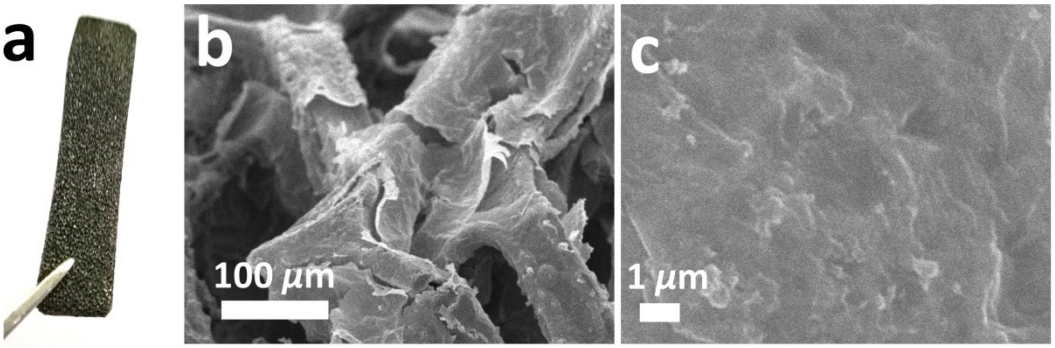

Figure S6. (a) Photo and (b, c) SEM images of the rGO@NiMn-LDH@NF electrode surface after cycling.

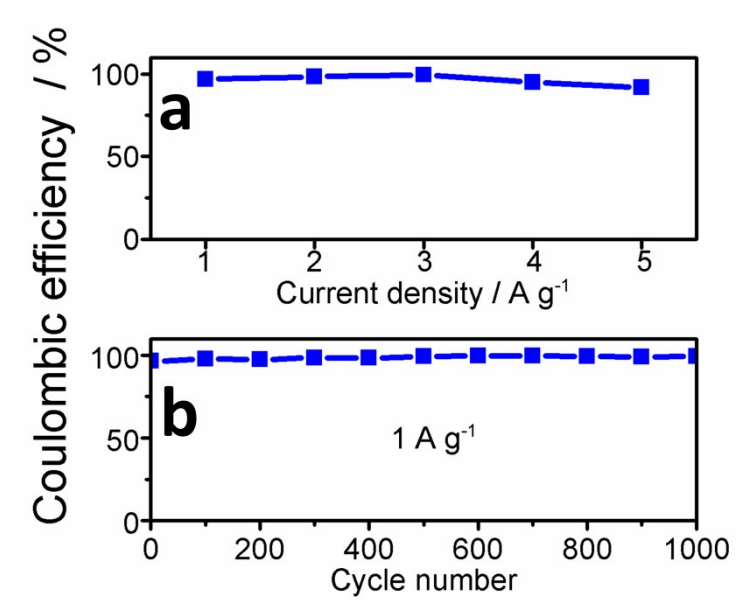

Figure S7. Coulombic efficiency of the ASC device as a function of (a) current densities and (b) cyclic numbers at 1 A g^{-1}.

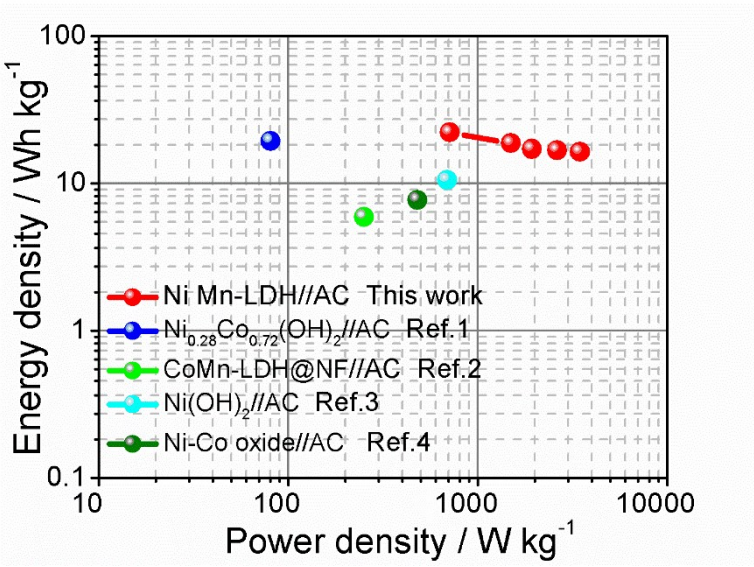

Figure S8. Energy and power densities of the ASC device. Below is the list of references:

1. Y. Tang, Y, Liu, S. Yu, W. Guo, S. Mu, H. Wang, Y. Zhao, L. Hou, Y. Fan, F. Gao, Electrochimica Acta, 2015, 161, 279-289.
2. A. D. Jagadale, G. Guan, X. Li, X. Du, X. Ma, X. Hao, A. Abudula, Journal of Power Sources, 2016, 306, 526-534.
3. J. Huang, P. Xu, D. Cao, X. Zhou, S. Yang, Y. Li, G. Wang, Journal of Power Sources, 2014, 246, 371-376.
4. L. Wang, D. Wang, X. Y. Dong, Z. J. Zhang, X. F. Pei, X. J. Chen, B. Chen and J. J. Jin, Chem. Commun., 2011, 47, 3556-3558

Supplementary Table

Table S1. Impedance parameters calculated from the equivalent circuit.

Electrodes	$R_s(\Omega)$	$R_{ct}(\Omega)$
rGO@NiMn-LDH@NF	0.61	0.91
NiMn-LDH@NF	1.44	16.66

Table S1. Comparison of capacitive performances in reported LDH electrodes.

Electrode materials	**Specific capacitance at 1 A g^{-1} (F g^{-1})**	**Year**	**Reference**
rGO@NiMn-LDH@NF	1696		This work
NiCo-LDH	1200	2018	1
CoAl-LDH/FGN	1222	2017	2
NiCo-LDH/CFC	2767	2017	3
NiMn-LDH/Porous carbon	*1634*	2017	4
GP@LDH	2395	2017	5
Ni-Co@Ni-Co LDH	*2200*	2017	6
Ti_3C_2/Ni-Co-Al-LDH	*748*	2017	7
rGO@MgAl-LDH	1334	2016	8
MXene/LDH	1061	2016	9
NiMn-LDH	1511	2016	10
CoMn LDH	1063	2016	11
CBC-N@LDH	1950	2016	12
MnCo-LDH@Ni $(OH)_2$	2320	2016	13
NiCo-LDH/CNTs	1151	2015	14
EG-Co-Ni LDH	1313	2015	15
3DCGNC	1760	2015	16
Co_3O_4@NiAl-LDHs	1772	2014	17
LDHs-Nps/CH-NWs	1297	2014	18
Ni-Co LDH hybrid film	2682	2013	19
GNS/LDH	781	2011	20

Reference

1 X. He, R. Li, J. Liu, Q. Liu, R. R. chen, D. Song and J. Wang, *Chem. Eng. J.*, 2018, **334**, 1573–1583.

2 W. Peng, H. Li and S. Song, *ACS Appl. Mater. Interfaces*.

3 T. Wang, S. Zhang, X. Yan, M. Lyu, L. Wang, J. Bell and H. Wang, *ACS Appl. Mater. Interfaces*, 2017, **9**, 15510–15524.
4 M. Yu, R. Liu, J. Liu, S. Li and Y. Ma, *Small*, 2017, **13**, 1–9.
5 D. Du, X. Wu, S. Li, Y. Zhang, W. Xing, L. Li, Q. Xue, P. Bai and Z. Yan, *J. Mater. Chem. A*, 2017, **5**, 8964–8971.
6 Y. Liu, N. Fu, G. Zhang, M. Xu, W. Lu, L. Zhou and H. Huang, *Adv. Funct. Mater.*, 2017, **27**, 1–11.
7 R. Zhao, M. Wang, D. Zhao, H. Li, C. Wang and L. Yin, *ACS Energy Lett.*, 2018, **3**, 132–140.
8 G. Hatui, G. C. Nayak and G. Udayabhanu, *Electrochim. Acta*, 2016, **219**, 214–226.
9 Y. Wang, H. Dou, J. Wang, B. Ding, Y. Xu, Z. Chang and X. Hao, *J. Power Sources*, 2016, **327**, 221–228.
10 X. L. Guo, X. Y. Liu, X. D. Hao, S. J. Zhu, F. Dong, Z. Q. Wen and Y. X. Zhang, *Electrochim. Acta*, 2016, **194**, 179–186.
11 A. D. Jagadale, G. Guan, X. Li, X. Du, X. Ma, X. Hao and A. Abudula, *J. Power Sources*, 2016, **306**, 526–534.
12 F. Lai, Y. E. Miao, L. Zuo, H. Lu, Y. Huang and T. Liu, *Small*, 2016, **12**, 3235–3244.
13 S. Liu, S. C. Lee, U. Patil, I. Shackery, S. Kang, K. Zhang, J. H. Park, K. Y. Chung and S. Chan Jun, *J. Mater. Chem. A*, 2017, **5**, 1043–1049.
14 M. Li, K. Y. Ma, J. P. Cheng, D. Lv and X. B. Zhang, *J. Power Sources*, 2015, **286**, 438–444.
15 C. Wang, X. Zhang, Z. Xu, X. Sun and Y. Ma, *ACS Appl. Mater. Interfaces*, 2015, **7**, 19601–19610.
16 M. Yang, H. Cheng, Y. Gu, Z. Sun, J. Hu, L. Cao, F. Lv, M. Li, W. Wang, Z. Wang, S. Wu, H. Liu and Z. Lu, *Nano Res.*, 2015, **8**, 2744–2754.
17 F. Ning, M. Shao, C. Zhang, S. Xu, M. Wei and X. Duan, *Nano Energy*, 2014, **7**, 134–142.
18 J. Yang, C. Yu, X. Fan and J. Qiu, *Adv. Energy Mater.*, 2014, **4**, 1–8.
19 H. Chen, L. Hu, M. Chen, Y. Yan and L. Wu, *Adv. Funct. Mater.*, 2014, **24**, 934–942.
20 Z. Gao, J. Wang, Z. Li, W. Yang, B. Wang, M. Hou, Y. He, Q. Liu, T. Mann, P. Yang, M. Zhang and L. Liu, *Chem. Mater.*, 2011, **23**, 3509–3516.